Distributed Flow Control using Embedded Sensor-Actuator Networks for the Reduction of Combined Sewer Overflow (CSO) Events

Pu Wan, Michael D. Lemmon

Abstract— **This paper studies the distributed control of network flows using an embedded sensor-actuator network. We focus on the problem of reducing the frequency of combined sewer overflow (CSO) events in city sewer systems. This is an important environmental problem whose cost effective solution is of great interest across the world. Our approach embeds microprocessor controlled sensors and actuators directly into the sewer network. These embedded processors communicate with other over a multi-hop communication network whose topology follows the topology of the sewer network. We use Pontryagin's maximum principle to develop a switching control where control decisions are made in a distributed manner. We present simulation results showing that the proposed method has the potential of greatly reducing the frequency of CSO events over existing passive thresholding strategies.**

I. Introduction

Embedded sensor-actuator networks consist of microprocessor controlled sensors and actuators that communicate with each other over multi-hop communication networks. In recent years there has been considerable interest in using such networks in pursuer-evader problems [1], cooperative acoustic localization in sensor networks [2], monitoring building structural integrity [3], mobile robotics [4], and sewer flow control [5]. This paper examines distributed control strategies for the sewer network application described in Ruggaber et al. [5].

Many early applications of sensor-actuator networks (e.g., [1], [2], [3], [4]) used actuation primarily to improve a sensor network's ability to detect events and estimate event parameters. These networks, however, can also be used to control large-scale interconnected systems. Examples of such applications include the electric power grid, supply chains, traffic networks, and wastewater networks. Sensor-actuator networks provide a convenient technology for realizing distributed control schemes that can greatly reduce the cost and complexity of the control implementation.

This is the motivation for Ruggaber er al.'s [5] use of sensor-actuator networks. Ruggaber's case study showed that sensor-actuator networks provide a cost effective technology for controlling sewer flows. The study, however, did not provide a control scheme that could be easily scaled up to an entire metropolitan area. The purpose of this paper is to develop a scalable distributed flow control strategy that can be implemented on an embedded sensor-actuator network to reduce the frequency of combined sewer overflow (CSO) events.

In the rest of this paper, we discuss the CSO problem (section II) and develop a simplified system model (section III) that is used to formulate an optimal control problem (section IV). A networked control strategy is developed (section V) which can be implemented in a distributed manner on a wireless sensor-actuator network (section VI). Simulations results (section VII) show that our control can signficantly reduce the frequency of CSO events.

Mr. Wan and Dr. Lemmon are with the department of Electrical Engineering, Univ. of Notre Dame, Notre Dame, IN 46556; e-mail: pwan,lemmon@nd.edu. The authors gratefully acknowledge the partial financial support of the Indiana 21st Century Research Fund, and the National Science Foundation (NSF-ECS04-00479). The authors would also like to acknowledge the generous technical support provided by Dr. Luis Montestruque and Mr Tim Ruggaber (EmNet LLC) with regard to the South Bend sewer system simulation models.

II. Combined-Sewer Overflow Problem

Nearly all U.S. cities in the Northeast and Midwest have sewer systems that combine sanitary and storm water flows in the same system. During rain storms, wastewater flows can easily overload these combined sewer systems, thereby causing operators to dump the excess water into the nearest river or stream. This discharge is called a combined sewer overflow (CSO) event [6]. The discharged water is highly impacted with biological and chemical contaminants, thereby, creating a major environmental hazard. Under the provisions of the 1974 clean water act, the environmental protection agency (EPA) has begun fining municipalities for CSO events. These fines are substantial, sometimes running into the tens of millions of dollars. Municipalities have therefore begun looking for cost-effective ways of reducing the frequency of CSO events.

The straightforward solution to the CSO problem is to enhance existing sewer infrastructure by separating storm and sanitary flows, increasing the capacity of the wastewater treatment plant (WWTP), or building large off-line storage reservoirs. All of these options are extremely expensive and highly distruptive to the community.

Another solution uses the excess storage capacity in a city's sewer to temporarily store water during a storm. This option is referred to as in-line storage. The economical and reliable control of CSO events through in-line storage requires real-time monitoring and control.

Current approaches to real-time monitoring and control of sewer systems do not scale well. Sensor data is usually collected by a single computer over a Supervisory Control And Data Acquisition (SCADA) network. The control is computed by a single computer and then distributed to the system through the SCADA network. It takes time to gather sensor data and this limits the rate at which control commands can be fed back to the system. The controls are

usually computed by solving a large-scale nonlinear optimal control problem [7] [8], a linear quadratic regulator problem [9], or a model predictive control (MPC) problem [10] [11]. Fuzzy logic controllers [12] have also been proposed. These algorithms, however, are all computed in a centralized fashion for a very high-order dynamical system. The system model is highly nonlinear with a significant amount of model uncertainty. As a result, centralized control of sewer systems tends to be complex, computationally intensive, and certainly not robust to modeling error. All of these factors conspire to limit the scalability of centralized approaches to sewer flow control.

A distributed approach to sewer control (CSOnet) was presented by Ruggaber et al. [5]. This case study used an embedded network of microprocessor controlled sensors and actuators to control CSO events. The network used a very simple local feedback scheme to control a stretch of sewer system fed by a 1500 foot wide by 3.2 mile long corridor. In its first month of service the network prevented a 2 million gallon CSO event. The cost of the deployed network was around $25,000, which is half of what it would cost using traditional SCADA network technologies.

The sensor-actuator network used by Ruggaber et al, therefore appears to provide a cost-effective solution for controlling small CSO events. The control used in that pilot study was a very simple switching law. A more sophisticated control strategy must be developed which can be scaled up to a metropolitan level in a manner that is competitive with commercial MPC control strategies. The following sections present a control that appears to be well-suited for distributed implementation on sensor-actuator networks.

III. Open Channel Flow

This section presents the fundamental equations that govern open channel flow. Simplifications are then made on those governing equations to obtain a simplified model for the plant to be controlled.

The flow of water within the sewer network is modelled as an *open channel flow*. The most frequently used model for unsteady and non-uniform open channel flow is the *complete dynamic wave model* [13]. This model consists of two equations: the continuity equation and the momentum equation. The *continuity equation* models the conservation of mass and is given as:

$$\frac{\partial A}{\partial t} + \frac{\partial Q}{\partial x} = 0. \tag{1}$$

where x is the spatial coordinate along the length of the pipe (m), t is time (s), Q is the flow (m^3/s), and A is the cross sectional area of the flow (m^2). Equation 1 says the mass of water is conserved along any closed contour in the $x-t$ plane. The *momentum equation* is

$$0 = gA\frac{\partial H}{\partial x} + \frac{\partial Q}{\partial t} - \sigma\left(2V\frac{\partial A}{\partial t} + V^2\frac{\partial A}{\partial x}\right) + gAS_f \tag{2}$$

where H is the water head level (height of water surface above the ground level) (m), $V = Q/A$ is the flow velocity (m/s), and g is the gravitational acceleration constant. The constant σ is a real number depending on the depth of the flow. S_f is called the *friction slope*, which is determined from *Manning's equation*

$$S_f = \frac{(n/1.49)^2}{AR^{4/3}}Q|V| \tag{3}$$

where n is a constant dependent on the roughness of the conduit and $R = A/P$ where P is the "wetted" perimeter of the pipe.

Equations 1-3 form a set of nonlinear partial differential equations (PDEs) that we call the complete dynamic wave model. It is difficult to derive controllers for systems characterized by PDEs, so we seek a simplified model which can be characterized by a set of nonlinear ordinary differential equations (ODEs). In particular, we adopt a steady (time invariant) and non-uniform (spatially variant) version of the momentum equation and an unsteady (time-varying) version of the continuity equation.

Let's consider a pipe of length L connecting two manholes as shown in figure 1. Assume that the flow rate, Q, is slowly varying. We can therefore neglect the partial derivatives, $\partial Q/\partial t$ and $\partial A/\partial t$, in equation 2 to obtain

$$\frac{\partial H}{\partial x} = \frac{H_d - H_u}{L}, \quad \frac{\partial A}{\partial x} = \frac{A_d - A_u}{L}$$

where L is the length of the pipe. H_u and H_d are the water head levels at the upstream and downstream manhole, respectively (see figure 1). A_u and A_d are the cross sectional flow areas upstream and downstream of the pipe. With these simplifications, the momentum equation can be reduced to an algebraic equation

$$H_u - H_d = kQ^2 \tag{4}$$

where k is

$$k = \frac{L(n/1.49)^2}{A^2R^{4/3}} - \sigma(A_d - A_u)\frac{1}{gA^3} \tag{5}$$

and A is the average cross sectional flow area in the pipe.

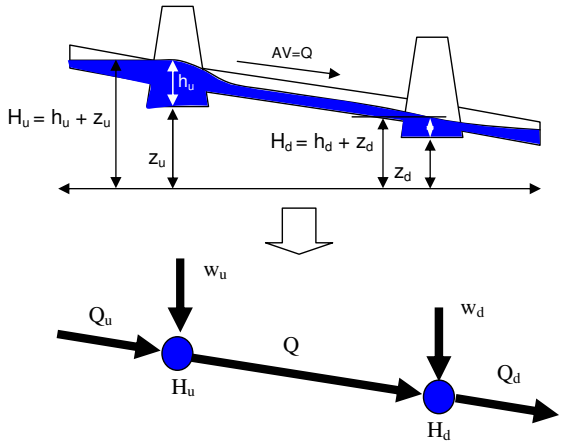

Fig. 1. Simplified Model for a Single Pipe

If we focus our attention on a single manhole (take the upstream manhole for example), then the continuity equation 1 can be rewritten as,

$$a_u \frac{dH_u}{dt} = \sum_{\text{in}} Q_{\text{in}} - \sum_{\text{out}} Q_{\text{out}} \tag{6}$$

where Q_{in} and Q_{out} are the flows that go into and out of the manhole, respectively. a_u is the water surface area of the manhole. Equation 6 simply says that the difference between inflows and outflows for a particular manhole is equal to the rate of change in water storage.

The water network shown on the top of figure 1 can be mapped to the graph shown at the bottom of figure 1. In this graph, the state of each node is given by the head level H at the manhole, and the state of each link is given by the flow Q in the pipe. In this figure, the continuity equation for the upstream node takes the form,

$$a_u \frac{dH_u}{dt} = Q_u - Q + w_u$$

where w_u is the inflow from the storm. Throughout this paper we'll refer to pipes as links and manholes as nodes. Our simplified model therefore consists of the ODEs and algebraic expressions given in equations 4-6. This simplified model was validated against a high-fidelity SWMM [**?**] model of the interceptor sewer system in South Bend, Indiana.

IV. Problem Formulation

This section formulates the problem of controlling CSO events as an optimal control problem. The problem statement is based on our simplified model in equations 4-6. We use a municipal interceptor sewer line to illustrate the problem. The methodology, however, can be extended to other network topologies.

Many municipal sewer systems are combined sewers that mix storm and sanitary flows. The trunk lines from the combined sewers are connected to a large *interceptor sewer*. The interceptor sewer intercepts flows from the combined sewer and directs these flows to a wastewater treatment plant (WWTP) where the flows are treated and released into the environment. The combined sewer trunk line and interceptor sewer connect at a *CSO diversion structure*. The CSO diversion structure is the point where we can apply control. Many current systems use a local thresholding control. When the depth of the flow exceeds a fixed preset threshold, the excess overflows into the river. Below this threshold, the flow is diverted into the interceptor sewer for subsequent treatment at the WWTP. The control strategy we propose using adjusts the amount of water diverted into the interceptor sewer based on a threshold that is a function of the system's current state.

The sewer system in figure 2 can be abstracted to a straight line of $N+1$ interconnected nodes, as shown in figure 3. The state of the link leaving the ith node is the flow Q_i. The state of the ith node along the line is the head level H_i for $i = 1, \ldots, N$. These N nodes represent the manholes along the interceptor sewer. The $N+1$st node in the system is

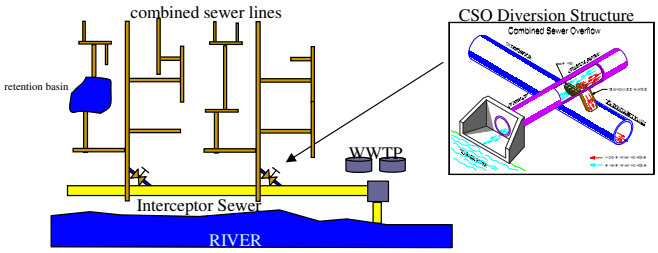

Fig. 2. South Bend Interceptor Sewer and CSO Diversion Structure

the WWTP, where its head level H_{N+1} is the ground level. Above each manhole node is a CSO diversion node. The flow entering this node is the external inflow w_i, the input from the old sewer lines (sanitary water, rainfall, etc). The two flows leaving each CSO diversion node are O_i the overflow dumped into the river (overflow) and u_i the flow diverted into the ith manhole node from the ith CSO diversion node. This diverted flow, u_i, represents our control variable.

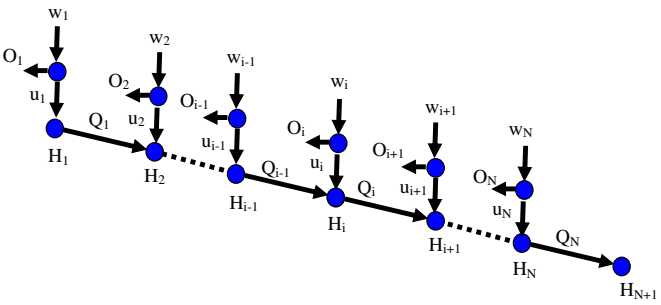

Fig. 3. Graph of South Bend Interceptor Sewer

Our control problem seeks to minimize the total overflow from all CSO diversion nodes subject to state constraints on the nodes/links and a maximum flow limit for the entire network. Minimizing the total overflow is equal to maximizing the total diverted flow. Our problem therefore seeks to maximize

$$J(u_1, \cdots, u_N) = \sum_{i=1}^{N} \int_0^{T_s} C_i u_i(\tau) d\tau \tag{7}$$

subject to

$$a_i(\tau)\frac{dH_i(\tau)}{dt} = u_i(\tau) + Q_{i-1}(\tau) - Q_i(\tau) \tag{8}$$

$$0 = H_i(\tau) - H_{i+1}(\tau) - k_i(\tau)Q_i^2(\tau) \tag{9}$$

$$0 \leq u_i(\tau) \leq w_i(\tau) \tag{10}$$

$$\overline{H}_i \geq H_i(\tau) \tag{11}$$

$$\overline{Q} \geq \sum_{j=1}^{N} u_j(\tau) \tag{12}$$

for $i = 1, \ldots, N$ and $\tau \in [0, T_s)$ where $Q_0(\tau) = 0$ and $H_{N+1}(\tau) = 0$. In equation 7, C_i is a set of weighting coefficients (costs), and T_s is the horizon (storm duration) over which to maximize the diverted flow. Equations 8-9

characterize the network's state variables. The optimization is done subject to the control being admissible (equation 10 and 12) and state constraints in equation 11. The constant $\overline{H}_i$ in equation 11 represents the head level when the manhole begins flooding. The constant $\overline{Q}$ represents a maximum flow limit for the entire network. This maximum flow limit may originate in limitations on the WWTP's capacity.

V. Optimal Controller

Rather than working directly with the objective in equation 7, we consider the finite horizon objective in which the nth $(n = 0, \cdots, \infty)$ optimal control problem tries to maximize

$$J_n(u_1, \cdots, u_N) = \sum_{i=1}^{N} \int_{t_n}^{t_n+T_n} C_i u_i(\tau) d\tau \tag{13}$$

subject to the constraints given above in equations 8-12. In this case, T_n represents a time horizon over which the nth problem's input flows $w_i(\tau)$ are nearly constant. The time $t_n = \sum_{i=0}^{n-1} T_i$ is the inital time for the nth problem. We assume $t_0 = 0$. This section uses Pontryagin's maximum principle as a necessary characterization of "optimal" controls. This characterization is then used to generate a distributed switching control strategy.

Assumption A1: The underlying assumption throughout this section is that the dynamics of the system in equations 8-9 are "slow". This assumption means over the interval $[t_n, t_n + T_n]$, the flow Q and storm inflows, w_i, vary slowly enough to be taken as constant.

Set of Admissible Controls: The problem's control lies in a bounded set of admissible controls. This occurs because the diverted flow, u_i, clearly cannot be larger than the storm inflow, w_i. Let $u = [u_1, \cdots, u_N] \in \Re^N$ denote the vector formed by the controls. At time $t \in \Re$ the control vector lies in an admissible set $U_t \subset \Re^N$ defined by

$$U_t = \left\{ u \in \Re^N \; : \; \begin{array}{l} \sum_{j=1}^{N} u_j \le \overline{Q} \\ 0 \le u_i \le w_i(t) \quad (i = 1, \ldots, N) \end{array} \right\} \tag{14}$$

where $\overline{Q}$ is the maximum flow capacity of the network.

Without loss of generality we assume $n = 0$ in equation 13 where $t_0 = 0$. Let's assume that $T = T_0$ is chosen so that none of the state constraints in equation 11 is active. The following theorem provides a simple necessary condition that must be satisfied by the optimal control u^* over this interval.

Theorem 5.1: Assume $\sum_{j=1}^{N} w_j(\tau) \ge \overline{Q}$ for all $\tau \in [0, T]$. Let $u^* : [0, T] \to \Re^N$ maximizes the finite-horizon objective in equation 13 subject to constraints in equations 8-12. Further assume that the constraints in equation 11 are not active under the optimal control $u^*(\tau)$ for any $\tau \in [0, T]$. Then for each $\tau \in [0, T]$, the optimal control solves the linear program

$$\begin{array}{ll} \text{maximize:} & \sum_{i=1}^{N} C_i u_i(\tau) \\ \text{subject to:} & u(\tau) \in U_\tau \end{array} \tag{15}$$

Proof: The problem's control Hamiltonian $\mathcal{H} : \Re^{3N} \to \Re$ is

$$\mathcal{H}(H, p, u) = \sum_{i=1}^{N} C_i u_i(\tau) + \sum_{i=1}^{N} p_i(\tau) f_i(H, u_i) \tag{16}$$

where

$$f_i(H, u_i) \;=\; \frac{1}{a_i}\left(u_i + Q_{i-1} - Q_i\right) \tag{17}$$

and $p_i : [0, T] \to \Re$ $(i = 1, \ldots, N)$ are the problem's costates. By Pontryagin's maximum principle (PMP) we know that u^* satisfies

$$u^*(\tau) = \arg\max_{u \in U_\tau} \sum_{i=1}^{N} \left(C_i + \frac{p_i(\tau)}{a_i} \right) u_i \tag{18}$$

At each time τ, the u^* in equation 18 is the solution to a linear program. To solve this problem we need to know the costate trajectory $p(\tau)$ for $\tau \in [0, T]$. The costate satisfies the differential equation

$$\dot{p}_i = \left\{ \begin{array}{ll} E_i p_i - F_i p_{i+1} & i = 1 \\ -E_{i-1} p_{i-1} + (F_{i-1} + E_i) p_i - F_i p_{i+1} & 1 < i < N \\ -E_{i-1} p_{i-1} + F_{i-1} p_i & i = N \end{array} \right. \tag{19}$$

where $E_i = \frac{1}{2 a_i k_i Q_i}$ and $F_i = \frac{1}{2 a_{i+1} k_i Q_i}$. Under assumption A1 the time interval T is short so that a_i, k_i, and Q_i are constants. The costate equation is therefore a linear differential equation. Because there is no terminal penalty in the objective function in equation 13, we know that $p_i(T) = 0$ for all i. The only way this can happen is if $p_i(\tau) = 0$ for all $\tau \in [0, T]$. The linear program in equation 18 therefore has the objective $\sum_{i=1}^{N} C_i u_i$, thereby completing the theorem's proof. ∎

We now consider the problem in which at least one of the state constraints in equation 11 is active.

Theorem 5.2: Assume $\sum_{j=1}^{N} w_j(\tau) \ge \overline{Q}$ for all $\tau \in [0, T]$. Let $u^* : [0, T] \to \Re^N$ maximizes the finite-horizon objective in equation 13 subject to constraints in equations 8-12. Let Q^* denote the flows under this optimal control. Let $\Omega \subset \{1, \cdots, N\}$ and assume for all $j \in \Omega$ that the state constraints in equation 11 are active. Then for each $\tau \in [0, T]$ the optimal control solves the linear program

$$\begin{array}{ll} \text{maximize:} & \sum_{i=1}^{N} C_i u_i(\tau) \\ \text{subject to:} & 0 \le u_i(\tau) \le w_i \quad (i \notin \Omega) \\ & u_j(\tau) = Q_j^*(\tau) - Q_{j-1}^*(\tau) \quad (j \in \Omega) \\ & \sum_{i=1}^{N} u_i(\tau) \le \overline{Q} \end{array} \tag{20}$$

Proof: The proof of this theorem is nearly identical to the proof in theorem 5.1 except that we use the version of Pontryagin's maximum principle that applies to state constraints. The costate in this case satisfy

$$\dot{p} = -\frac{\partial \mathcal{H}}{\partial x} + \sum_{j \in \Omega} \lambda_j \frac{\partial f_j(H^*, u_j)}{\partial x} \tag{21}$$

where λ_j is a Lagrange multiplier associated with the constraint $f_j(H^*, u_j) = 0$. By the maximum principle we require that u^* satisfy equation 18 subject to the constraint that $f_j(H^*, u_j) = 0$ for those nodes whose state constraint is active. Requiring $f_j(H^*, u_j) = 0$ for $j \in \Omega$, is the same as requiring $u_j = Q_j^* - Q_{j-1}^*$, which gives the second constraint in the linear program. Under assumption A1, we approximate Q^* as constant in the interval. This enable us to write $f_j(H^*, u_j) = f_j(u_j)$. In this way the second term on the right side of the costate equation is zero, and we have

the exact same costate equation as in equation 19. Since we also have $p_i(T) = 0$ for all i, the rest of the proof follows the same as theorem 5.1, which completes the proof. ■

Theorems 5.1 and 5.2 both suggest that $u^*(\tau)$ will lie on the boundary of the admissible set, U_τ, of controls. The following theorem shows that the optimal control must be a switching control.

Theorem 5.3: Let $u^* : [0,T] \rightarrow \Re^N$ be the optimal control for the problem in theorem 5.1. If the costs C_i are all distinct, and can be ordered as $C_{i_{j+1}} < C_{i_j}$ for $j = 1, \ldots, N-1$, then for each $\tau \in [0,T]$ there exists a $r \in \{1, \ldots, N\}$ such that

$$u^*_{i_j}(\tau) = \begin{cases} w_{i_j}(\tau) & 1 \le j \le r-1 \\ \overline{Q} - \sum_{k=1}^{r-1} w_{i_k}(\tau) & j = r \\ 0 & r+1 \le j \le N \end{cases} \quad (22)$$

Proof: We will use the Karush-Kuhn-Tucker (KKT) condition to prove the theorem. For simplicity, we will use u^* and w instead of $u^*(\tau)$ and $w(\tau)$ in the proof.
Define

$$\begin{aligned} L(u^*, \lambda, \mu, \nu) &= \sum_{j=1}^{N} C_{i_j} u^*_{i_j} + \lambda \left(\sum_{j=1}^{N} u^*_{i_j} - \overline{Q} \right) \\ &\quad + \sum_{j=1}^{N} \mu_{i_j}(-u^*_{i_j}) + \sum_{j=1}^{N} \nu_{i_j}(u^*_{i_j} - w_{i_j}) \end{aligned}$$

where for $j = 1, \ldots, N$

$$\begin{array}{lll} \lambda \le 0, & \sum_j u^*_{i_j} - \overline{Q} \le 0, & \lambda(\sum_j u^*_{i_j} - \overline{Q}) = 0 \\ \mu_{i_j} \le 0, & -u^*_{i_j} \le 0, & \mu_{i_j}(-u^*_{i_j}) = 0 \\ \nu_{i_j} \le 0, & u^*_{i_j} - w_{i_j} \le 0, & \nu_{i_j}(u^*_{i_j} - w_{i_j}) = 0 \end{array} \quad (23)$$

Since u^* is optimal, we have

$$\frac{\partial L}{\partial u^*_{i_j}} = C_{i_j} + \lambda - \mu_{i_j} + \nu_{i_j} = 0, \quad j = 1, \ldots, N \quad (24)$$

We first show by contradiction that the constraint

$$\sum_{j=1}^{N} u^*_{i_j} - \overline{Q} \le 0,$$

is active. Assume this constraint is not active. This means $\lambda = 0$, which implies $C_{i_j} = \mu_{i_j} - \nu_{i_j}$ for all j. By equation 23, μ_{i_j} and ν_{i_j} are either both 0 (if $0 < u^*_{i_j} < w_{i_j}$), or one is 0 and the other is nonpositive (if $u^*_{i_j} = 0$ or $u^*_{i_j} = w_{i_j}$). Since $C_{i_j} > 0$, this implies that $\mu_{i_j} = 0$, and $\nu_{i_j} < 0$. We can therefore conclude that $u^*_{i_j} = w_{i_j}$ for all j, which implies $\sum_{j=1}^{N} u^*_{i_j} = \sum_{j=1}^{N} w_{i_j} \ge \overline{Q}$. This contradicts the assumption that the constraint is not active.

We next show there exists at most one r such that $0 < u^*_{i_r} < w_{i_r}$. Assume that there exists two, say $u^*_{i_r}$ and $u^*_{i_m}$. From equation 23, we have $\mu_{i_r} = \nu_{i_r} = \mu_{i_m} = \nu_{i_m} = 0$. This means $\lambda = -C_{i_r} = -C_{i_m}$ which contradicts the assumption that the coefficients C_i are distinct.

Finally let's assume there exists one r that $0 < u^*_{i_r} < w_{i_r}$, then $\mu_{i_r} = \nu_{i_r} = 0$ so that $\lambda = -C_{i_r}$ from equation 24. Applying equation 24 to $j \neq r$, yields $C_{i_j} - C_{i_r} = \mu_{i_j} - \nu_{i_j}$. It is easily shown that if $C_{i_j} > C_{i_r}$, then $u^*_{i_j} = w_{i_j}$. Furthermore if $C_{i_j} < C_{i_r}$, then $u^*_{i_j} = 0$. This means there exists a $r \in \{1, \ldots, N\}$ such that the optimal control u^* is given by equation 22. ■

Remark: The theorem says that the order of the costs C_i is the same as the order of nodes being chosen to divert flow. If we have $C_{i_{j+1}} < C_{i_j}$, then node i_1 will divert w_{i_1}, and node i_2 will divert w_{i_2}, until there comes a node i_r. Node i_r can't divert w_{i_r} because that will violate the capacity limit $\overline{Q}$, so it can only divert $\overline{Q} - \sum_{k=1}^{r-1} w_{i_k}$ to make sure the limit is satisfied. Then for $j > r$, node i_j can't divert any flow since the WWTP limit constraint is already active.

If some of the state constraints are active, as stated in theorem 5.2, then we will have $u^*_j(\tau) = Q^*_j(\tau) - Q^*_{j-1}(\tau)$ for $j \in \Omega$. For $j \notin \Omega$, $u^*_j(\tau)$ will follow the same as in theorem 5.3. This means one of them will satisfy $0 < u^*_j(\tau) < w_j(\tau)$, and the others are either 0 or $w_j(\tau)$.

If C_i are not all distinct, the optimal control u^* might not be unique. This happens when there exists a m that $C_{i_r} = C_{i_m}$, which means we can pick either node i_r or i_m to divert the amount of $\overline{Q} - \sum_{k=1}^{r-1} w_{i_k}(\tau)$, or we can share this amount of flow among them. In this case, the solution given by equation 22 is still one of the optimal controls.

Theorem 5.3 gives a switching control rule. For each node, the control input is either "full on" or "full off", with the exception of one node chosen to ensure the constraint $\sum_{j=1}^{N} u_j = \overline{Q}$ is active. The strategy is slightly modified when some of the state constraints are active. This modification is detailed below.

We assume that the costs C_i are all distinct, and can be ordered as $C_{i_{j+1}} < C_{i_j}$ for $j = 1, \ldots, N-1$. At a given time instant t each node i_j chooses u_{i_j}. This selection falls into one of two cases.

- In the first case, node i_j hits its state constraint $H_{i_j} = \overline{H}_{i_j}$ so that $i_j \in \Omega$. When this happens, node i_j sets its control to

$$u_{i_j} = Q_{i_j} - Q_{i_j - 1} \quad (25)$$

- In the second case, node i_j does not hit the state constraint so that $i_j \notin \Omega$. This node then selects u_{i_j} according to the following rule.

$$u_{i_j} = \begin{cases} w_{i_j} & \widetilde{Q} - W \ge w_{i_j} \\ \widetilde{Q} - W & 0 < \widetilde{Q} - W < w_{i_j} \\ 0 & \widetilde{Q} = W \end{cases} \quad (26)$$

where

$$\widetilde{Q} = \overline{Q} - \sum_{i_j \in \Omega} (Q_{i_j} - Q_{i_j - 1}), W = \sum_{i_k \notin \Omega, k=1}^{j-1} u_{i_k} \quad (27)$$

$\widetilde{Q}$ is the total free capacity for node $i_j \notin \Omega$ and W is the total used capacity for node $i_j \notin \Omega$. Note that if Ω is an empty set, then the control rule simplifies to equation 22.

Equation 25 and 26 describe a rule that nodes use to select their control actions. We now need to characterize those time instants, t, when the control rules are applied. We

can identify two distinctly different types of time instants. If node i's state constraint is active, then it will need to acquire real-time data about the flows Q_i and Q_{i-1}. This node's control would therefore need to be updated at a periodic rate which for this class of applications is on the order of $10-30$ seconds. The other type of decision time occurs at nodes that have not hit their state constraints. The control decision made by these nodes is essentially a switching decision (open or close the valve) and this only needs to change when the "discrete-state" (i.e. the set of active state constraints Ω) or the storm inflow w changes. In practice, the storm inflows and state constraint set Ω change slowly over time. This set of decision times tends to be a low rate aperiodic stream of times.

VI. Sensor-Actuator Network Implementation

Traditional CSO control systems have been implemented in a centralized manner over SCADA networks. Following the pilot study described by Ruggaber et al. [5], a sensor-actuator network implementation of our switching control strategy may be very beneficial. This section describes the sensor-actuator network used by Ruggaber et al. and discusses how our CSO control strategy could be implemented on this network in a way that requires very little communication.

Ruggaber's sensor actuator network (CSOnet) is an embedded network consisting of microprocessors controlling sensing and actuation devices embedded within the sewer system. Each computational node within CSOnet consists of at least three basic subsystems; the sensor/actuation subsystem, the processor module, and the wireless communication subsystem. The processor module is either a microprocessor or embedded single board computer that is interfaced to sensors and actuators through the sensor/actuation subsystem. The processor module can store sensor information locally and make control decisions based on information it receives from sensors and its wireless communication subsystem. The radio subsystem uses a low power radio that allow devices to communicate directly with each other by relaying data through other intermediary devices. This differs from traditional radio modem approaches in which each device communicates directly with a central controller, usually located at the WWTP.

CSOnet consists of three types of embedded nodes which we refer to as the gateway (Gnode), the instrument node (Inode), and the routing node (Rnode). The Inode and Rnode are both based on a commercial sensor network module (designed and produced by EmNet LLC). This node is a ruggedized modification of the U.C. Berkeley MICA2 node. It was designed to use a more powerful radio (2-4 km range) with more rugged power supplies and sensor interface hardware. The difference between the Inode and Rnode is that the Inode has a sensor subsystem, whereas the Rnode requires no such subsystem since it is only used to relay information. The Gnode is a single board embedded computer that can connect to the Internet. It has an actuator interface for controlling valves in the sewer network. In practice, Inodes gather data about head level and flow rates within the sewer system, Rnodes relay that sensor data to Gnodes and the Gnodes then compute the required control and actuates valves within the network to adjust local flow rates within the sewer system.

Figure 4 graphically illustrates CSOnet's deployment along an interceptor sewer similar to that shown in figure 2. In this figure, the CSOnet nodes are depicted as a square block with a letter inside it and a radio antenna. The letter inside the block indicates whether the CSOnet node is an Rnode (R), Gnode (G), or Inode (I). This deployment places Inodes in the interceptor sewer's manholes. These Inodes measure the head level in the interceptor sewer's manhole. Additional sensors also measure the flows entering and leaving the manhole. Gnodes are emplaced at the CSO diversion structure in the manhole connecting the diversion pipe to the combined sewer trunk line. These nodes measure the total combined sewer inflow. The Gnodes also actuate valves diverting water from the trunk line into the interceptor sewer. Rnodes are deployed between the CSO diversion structures and relay data between the CSO diversion structures in a multi-hop manner. In practice, Rnodes are placed above street level on light fixtures and traffic lights owned by the local municipality. Special antennas are used to transmit messages from Inodes (located within manholes below the street) to Gnodes and Rnodes (usually located above the street).

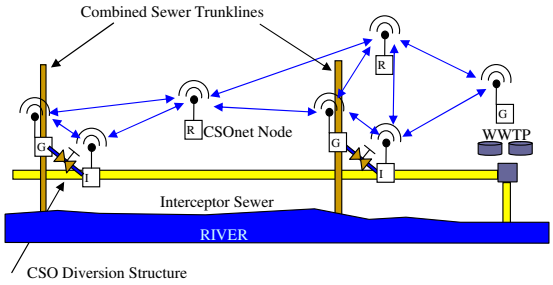

Fig. 4. CSOnet Deployment along Interceptor Sewer

The switching control strategy described in section V can be implemented in a *distributed* way on CSOnet. By a distributed implementation, we mean that decision making is distributed to the CSOnet nodes so that the ith node's diverted flow, u_i, is decided by the Gnode at that diversion point.

CSOnet's mesh communication network will need to support three different types of traffic. In the following, recall that the set $\Omega \subset \{1,\ldots,N\}$ is the set of nodes with active state constraints. Ω^c denotes the complement of Ω and contains all nodes with inactive state constraints. Associated with Ω^c is a sequence $\{i_j\}_{j=1}^{M}$ where $M = |\Omega^c|$. This sequence orders the nodes with inactive state constraints in order of decreasing cost. In other words, $C_{i_j} > C_{i_{j+1}}$ for $j = 1,\ldots,M-1$. The three classes are itemized below.

Traffic Class C1: The first class of traffic is used by

node $i \in \Omega$ (i.e. its state constraint is active). This traffic flow is periodic. The traffic originates in node i's immediate upstream (node $i-1$) and downstream (node $i+1$) neighbors and terminates at node i. Node i uses this information to compute its control u_i according to equation 25. This traffic stream is usually periodic. Simulation results suggest a period of $10 - 30$ seconds for real-life sewer system applications.

Traffic Class C2: The second class of traffic is used by any node i to transmit control decision to the node $i_1 \in \Omega^c$ (i.e. the node with the greatest cost coefficient). Messages in this traffic class are transmitted whenever node i's control level, u_i, changes by a set amount or whenever the node "changes" its status (i.e. it enters or leaves the set Ω). If node i has an active state constraint, its control level may change due to variations in the upstream and downstream flows, Q_i and Q_{i-1}. If node i has an inactive state constraint, its control level may change due to variations in the input storm flow w_i. The traffic stream, therefore, is aperiodic and event driven. Simulation results show that message transmission would be triggered on the order of every 1-10 minutes in real-life applications.

Traffic Class C3: The third class of traffic is used by nodes in Ω^c (i.e. state constraint is inactive). Messages of class C3 are triggered when node i_1 receives a class C2 mesage from a node in Ω. Upon receipt of the C2 message, node i_1 computes its control using equation 26. Node i_1 then transmits the quantity $\tilde{Q} - u_{i_1}$ to node i_2, the node in Ω^c with the next highest cost coefficient. Node i_2 then computes its control and transmits $\tilde{Q} - \sum_{j=1}^{2} u_{i_j}$ to node i_3. Node i_3 repeats the process. In general the rth node in the chain (node i_r) transmits the information $\tilde{Q} - \sum_{j=1}^{r} u_{i_j}$ to the next node $i_{r+1} \in \Omega^c$. This process continues until all nodes in Ω have updated their controls. Note that this third traffic class is also triggered in an aperiodic manner by the arrival of a class C2 message at node i_1.

Note that messages in traffic class C1 are generated at a relatively fast rate. However class C1 messages are only transmitted over a single hop, so that the total distance travelled by the messages is short. Let's define the traffic stream's "energy" as the transmission rate (msg/s) times the "distance" travelled (hops). Since we only have to transmit over a single hop, the overall energy in the C1 traffic stream is small. Messages in traffic class C2 and C3, however, may be transmitted between distant nodes. These traffic streams, however, are event driven and simulations suggest that average arrival rate of such messages is on the order of minutes rather than seconds. This suggests that the "energy" in traffic streams C2 and C3 is also relatively low.

The preceding discussion suggests that if we measure the communication network's work load in terms of the "energy" of its traffic streams, then our distributed control algorithm may require relatively little work. There is good reason to suspect that this work is significantly less than the work required by SCADA networks in implementing centralized MPC control schemes. Future work is being done to quantify how large the actual difference will be.

VII. Simulation Results

This section presents simulation results of our controller on a high-fidelity model of the 7-node interceptor sewer shown in figure 5 and the 36 node interceptor sewer of the city of South Bend, Indiana.

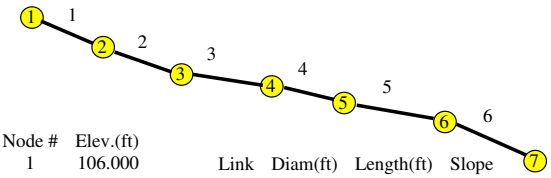

Node #	Elev.(ft)
1	106.000
2	103.000
3	100.000
4	98.608
5	98.257
6	97.581
7	95.813

Link	Diam(ft)	Length(ft)	Slope
1	2.5	700	.0043
2	3.5	1000	.0030
3	4.5	580	.0024
4	5	530	.0007
5	6	690	.001
6	6.5	520	.0034

Fig. 5. 7-node Interceptor Sewer used in Simulation

In this simulation, the parameters are listed in the following table. For the passive thresholding strategy, the fixed threshold is 40 (we only allow a maximum $40(cfs)$ flow into the interceptor line at each diversion structure). The external inflow is a rain event that last for 12 hours. The $40(cfs)$ threshold was chosen so that if all lines into the interceptor sewer exceeded this rate, then the interceptor sewer would flood. This is a commonly used criteria by which many real-life water districts set their CSO thresholds.

N	$T_s(min)$	$\overline{Q}(cfs)$	C
6	720	280	$[1.5, 1.4, 1.3, 1.2, 1.1, 1]^T$
$\overline{H}(ft) = [108.50, 105.50, 103.50, 103.11, 103.26, 103.58]^T$			

TABLE I
Simulation Parameters

Figure 6 plots the head levels of node 2 and 3 as a function of time (The dotted lines are the corresponding $\overline{H}_2$ and $\overline{H}_3$). It shows that the head constraints $H_2(t) \leq \overline{H}_2$ and $H_3(t) \leq \overline{H}_3$ are satisfied for all t, while each of them becomes active over some horizon. This means no flooding occurs during the rain event (Head levels at other nodes are always below the maximum level, and are not plotted here).

Figure 7 has five curves on it. They plot the time history of different flows. The one on top is the total rain flow. The straight line below it represents the WWTP capacity limit. The third curve, which lies right below the straight line, is the flow (Q_6) into the WWTP when our control is used. As we can see, the flow is always less or equal to the WWTP capacity limit. The fourth and fifth curve represent the total overflow when the passive thresholding strategy and our control is applied, respectively. The overflow under our control is significantly less than the other case. When the passive thresholding strategy is used, the total overflow is $2.6061 \times 10^6 (ft^3)$. The overflow drops to $5.4549 \times 10^5 (ft^3)$ when our control is applied. This is a decrease of 79.1%.

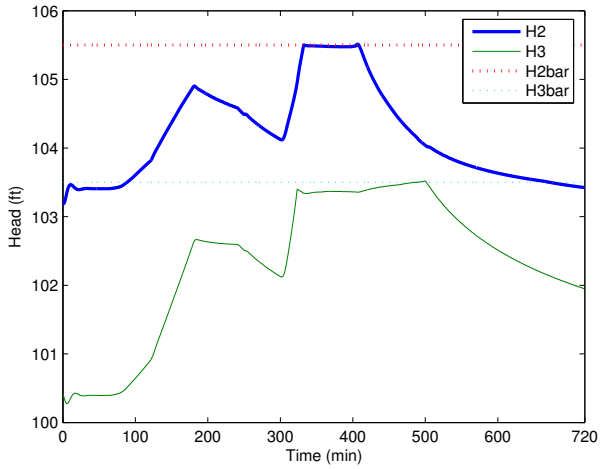

Fig. 6. Head level when using our control

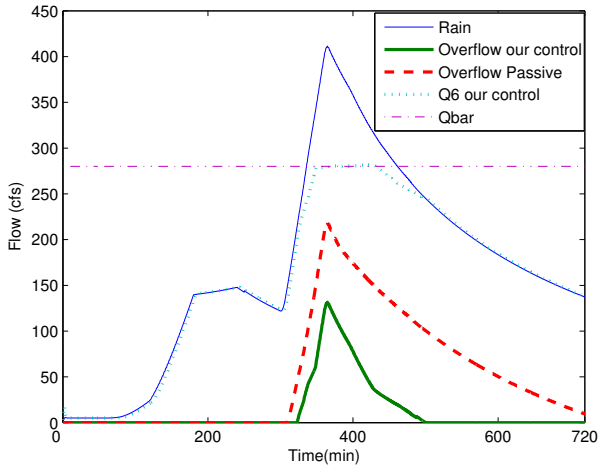

Fig. 7. Overflow comparison using our control vs passive thresholding

The algorithm was also simulated on the real South Bend interceptor sewer line which consists of 36 CSO diversion structures. The following three different storm scenarios are considered. Each storm drops rain nonuniformly over the city and moving from west to east over city at 20mph.

- S1. 0.485 inch of rain in 11 hours
- S2. 0.799 inch of rain in 13 hours
- S3. 2.046 inch of rain in 19 hours

The simulation results are given in table II. It shows the existing system overflow (using fixed thresholding strategy), controlled system overflow (when implementing our control scheme), and overflow decrease in percentage obtained by our control scheme over South Bend's existing CSO system. You can see from the table that our proposed approach reduces the total storm overflow by $24\% - 40\%$, which is significant.

Storm	existing overflow ($ft^3 \times 10^6$)	controlled overflow ($ft^3 \times 10^6$)	overflow decrease
S1	0.46	0.28	40%
S2	2.51	1.90	24%
S3	6.04	3.79	37%

TABLE II
OVERFLOW COMPARISON

VIII. SUMMARY

This paper studied a novel application of sensor-actuator networks to flow control in sewer networks. This is an important problem whose cost effective solution will have a major societal impact. We developed a switching control strategy that lends itself for distributed implementation on a sensor-actuator network. Simulations based on realistic models of municipal sewer systems indicate that our approach has the potential for greatly reducing the total combined sewer overflow. Future work will use recent funding from Indiana's 21st Century Research Fund to build and evaluate a metropolitan scale version of CSOnet using the control strategies introduced in this paper.

REFERENCES

[1] B. Sinpoli, C. Sharp, L. Schenato, S. Schaffert, and S. Sastry, "Distributed control applications with sensor networks," *Proceedings of the IEEE*, vol. 91, no. 8, pp. 1234–1246, 2003.
[2] C. Savarese, J. Rabaey, and J. Beutel, "Location in ad hoc wireless sensor networks," in *Proceedings of the IEEE Conference on Acoustics, Speech, and Signal Processing*, 2001.
[3] J.-B. Ihn and F.-K. Chang, "Detection and monitoring of hidden fatique crack growth using a built in piezoelectric sensor/actuator network: I. diagnostics," *Smart Materials and Structures*, vol. 13, pp. 609–620, 2004.
[4] G. Sibley, M. Rahimi, and G. Sukhatme, "Robomote: A tiny mobile robot platform for large scale sensor networks," in *Proceedings of IEEE International Conference on Robotics and Automation (ICRA)*, 2002.
[5] T. Ruggaber, J. Talley, and L. Montestruque, "Using embedded sensor networks to monitor, control, and reduce cso events: A pilot study," *Environmental Engineering Science*, vol. 24, no. 2, pp. 172–182, 2007.
[6] M. Schutze, A. Campisano, H. Colas, W. Schilling, and P. A. Vanrolleghem, "Real time control of urban wastewater systems; where do we stand today?" *Journal of Hydrology*, vol. 299, pp. 335–348, 2004.
[7] M. Marinaki and M. Papageorgiou, "Central Flow Control in Sewer Networks," *Journal of Water Resources Planning and Management*, vol. 123, no. 5, pp. 274–283, 1997.
[8] ——, "A non-linear optimal control approach to central sewer network flow control," *International Journal of Control*, vol. 72, no. 5, pp. 418–429, 1999.
[9] M. Marinaki, M. Papageorgiou, and A. Messmer, "Multivariable Regulator Approach to Sewer Network Flow Control," *Journal of Environmental Engineering*, vol. 125, no. 3, pp. 267–276, 1999.
[10] S. Duchesne, A. Mailhot, and J. Villeneuve, "Global Predictive Real-Time Control of Sewers Allowing Surcharged Flows," *Journal of Environmental Engineering*, vol. 130, no. 5, pp. 526–534, 2004.
[11] G. Cembrano, J. Quevedo, M. Salamero, V. Puig, J. Figueras, and J. Marti, "Optimal control of urban drainage systems. A case study," *Control Engineering Practice*, vol. 12, no. 1, pp. 1–9, 2004.
[12] K. Klepiszewski and T. Schmitt, "Comparison of conventional rule based flow control with control processes based on fuzzy logic in a combined sewer system," *Water Sci Technol.*, vol. 46, no. 6, pp. 77–84, 2002.
[13] M. Chaudhry, *Open Channel Flow*. Prentice-Hall, 1993.
[14] E. P. Agency, "Storm water management model (swmm)," http://www.epa.gov, March, 2007.